JACS
JOURNAL OF THE AMERICAN CHEMICAL SOCIETY
Communication
pubs.acs.org/JACS

Giant Negative Thermal Expansion in Bonded MnCoGe-Based Compounds with Ni_2In-Type Hexagonal Structure

Ying-Ying Zhao,[†] Feng-Xia Hu,*[,†] Li-Fu Bao,[†] Jing Wang,*[,†] Hui Wu,[‡,§] Qing-Zhen Huang,[‡] Rong-Rong Wu,[†] Yao Liu,[†] Fei-Ran Shen,[†] Hao Kuang,[†] Ming Zhang,[†] Wen-Liang Zuo,[†] Xin-Qi Zheng,[†] Ji-Rong Sun,[†] and Bao-Gen Shen[†]

[†]Beijing National Laboratory for Condensed Matter Physics and State Key Laboratory of Magnetism, Institute of Physics, Chinese Academy of Sciences, Beijing 100190, P. R. China

[‡]NIST Center for Neutron Research, National Institute of Standards and Technology, Gaithersburg, Maryland 20899, United States

[§]Department of Materials Science and Engineering, University of Maryland, College Park, Maryland 20742-2115, United States

Supporting Information

ABSTRACT: MnCoGe-based compounds undergo a giant negative thermal expansion (NTE) during the martensitic structural transition from Ni_2In-type hexagonal to TiNiSi-type orthorhombic structure. High-resolution neutron diffraction experiments revealed that the expansion of unit cell volume can be as large as $\Delta V/V \sim 3.9\%$. The optimized compositions with concurrent magnetic and structural transitions have been studied for magnetocaloric effect. However, these materials have not been considered as NTE materials partially due to the limited temperature window of phase transition. The as-prepared MnCoGe-based compounds are quite brittle and naturally collapse into powders. By using a few percents (3−4%) of epoxy to bond the powders, we introduced residual stress in the bonded samples and thus realized the broadening of structural transition by utilizing the specific characteristics of lattice softening enforced by the stress. As a result, giant NTE (not only the linear NTE coefficient α but also the operation-temperature window) has been achieved. For example, the average $\bar{\alpha}$ as much as -51.5×10^{-6}/K with an operating temperature window as wide as 210 K from 122 to 332 K has been observed in a bonded $MnCo_{0.98}Cr_{0.02}Ge$ compound. Moreover, in the region between 250 and 305 K near room temperature, the α value (-119×10^{-6}/K) remains nearly independent of temperature. Such an excellent performance exceeds that of most other materials reported previously, suggesting it can potentially be used as a NTE material, particularly for compensating the materials with large positive thermal expansions.

An increasing attention has been attracted to the materials with negative thermal expansion (NTE) due to the urgent demand in industries. In many cases, such as optical fiber reflective grating devices, high-precision optical mirrors, printed circuit boards, and machinery parts, a precisely tailored thermal expansion or even zero expansion is generally required. However, the overwhelming majority of materials show positive thermal expansion (PTE). By forming composites of NTE and PTE materials, an accurate coefficient of thermal expansion (CTE) can be achieved, thus developing NTE materials with various CTE as compensators has become an important challenge to meet the rapid requirements in highly advanced industries. In the past years, great efforts have made with several kinds of materials being identified as useful NTE materials, including the well-known ZrW_2O_8 family,[1] ScF_3,[2] CuO nanoparticles,[3] $PbTiO_3$-based compounds,[4] $(Bi,La)NiO_3$,[5] antiperovskite manganese nitrides,[6−10] and $La(Fe,Co,Si)_{13}$ compounds.[11] However, only a few have been used in practice due to the limited NTE coefficient, narrow temperature window, and poor mechanical properties as well as the low electrical conducting characteristics.

Recently, the ternary metallic compounds MM′X with hexagonal Ni_2In-type structure have attracted much attention due to their rich magnetic and structural properties.[12−15] As a member of MM′X family, the stoichiometric MnCoGe alloy displays ferromagnetic properties with Curie temperature T_C at ∼345 K.[12] In the paramagnetic region the alloy undergoes a martensitic structural transition around $T_{stru} \sim 420$ K from the Ni_2In-type hexagonal structure (space group $P6_3/mmc$) to the TiNiSi-type orthorhombic structure (space group $Pnma$), which is accompanied by a pronounced lattice expansion upon cooling. More attractively, the crystallographic transition is sensitive to chemical and physical pressures. The optimized compositions with concurrent magnetic and structural transitions showing a large magnetocaloric effect have been discovered.

However, these materials have not been considered as NTE materials for practical applications up to now, though they surely display pronounced negative lattice expansion due to the martensitic structural transition. High-resolution neutron diffraction experiments revealed that the negative expansion of the unit cell volume during the martensitic structural transition can be as large as $\Delta V/V \sim -3.9\%$, but the temperature window of phase transition is limited. The as-prepared MnCoGe-based compounds are quite brittle and naturally fragment into powders. It is known that the NTE materials, as compensators, were usually made into powders and mixed with PTE materials, eventually achieving the precise CTE. Here, we introduce a few percents (3−4%) of epoxy to bond the powders and utilize the significant broadening of phase transition enforced by residual

Received: October 28, 2014
Published: January 28, 2015

DOI: 10.1021/ja510693a
J. Am. Chem. Soc. 2015, 137, 1746−1749

stress; giant linear NTE in a wide temperature window was obtained for a number of compositions. For example, the linear NTE coefficient $\bar{\alpha}$ as much as -51.5×10^{-6}/K with a temperature window as wide as 210 K from 122 to 332 K has been observed in a bonded $MnCo_{0.98}Cr_{0.02}Ge$ compound. Moreover, in the region between 250 and 305 K near room temperature, the α value (-119×10^{-6}/K) remains nearly independent of temperature. Such an excellent performance exceeds that of most other NTE materials reported previously. More attractively, high strength can be achieved by controlling the preparation arts during bonding process. The compressive strength can be as high as 70.4 MPa when a pressure of 11.5kbar was used during bonding process. Furthermore, electrical conducting properties of the bonded alloys can also be adjusted through choosing suitable binders.

The employed MnCoGe-based alloys in the present investigations, such as $Mn_{1-x}In_xCoGe$, $Mn_{1-x}Ni_xCoGe$, $MnCo_{1-x}Cr_xGe$, $MnCoGe_{1-x}Sb_x$, $MnCoGe_{1-x}In_x$, $MnCoGe_x$, and $MnCoGe_{1-x}Ga_x$, were prepared by an arc-melting technique, followed by annealing at 875 K for 6 days, and then cooling down to room temperature in oven. We found that all the as-prepared samples have naturally cracked into powders after annealing. A few epoxy plus hardening agent, totally 3−4 wt %, (or silver epoxy plus hardening agent, 6 wt % in total) was introduced and evenly mixed with the powders. The mixtures were molded under pressure and then solidified at 170 °C, eventually resulted in the bonded alloys (details can be found in the Supporting Information (SI)). The linear thermal expansion data ($\Delta L/L$) were measured using high-resolution strain gauge with a cooling rate of 2 K/min. Magnetic and electrical transport measurements were performed using a superconducting quantum interference magnetometer (SQUID-VSM). The neutron powder diffraction (NPD) experiments were performed at the NIST Center for Neutron Research on the BT-1 high-resolution neutron powder diffractometer. The crystal and magnetic structures were refined by the Rietveld method using the General Structure Analysis System (GSAS) suite of programs.[16]

Previous investigations and our recent studies indicated that, in MnCoGe, the replacement of Mn by In or Ni, Co by Cr, Ge by Sb, In, Ga, or vacancies can all shift the martensitic structural transition, T_{stru}, to low temperatures. As a result, the transition occurs between ferromagnetic (FM) martensitic and paramagnetic (PM) austenitic phases at some optimized compositions, such as $Mn_{1-x}In_xCoGe$ ($0.01 \le x \le 0.02$), $Mn_{1-x}Cr_xCoGe$ ($0.04 \le x < 0.27$),[14] $MnCoGe_{1-x}Sb_x$ ($0.01 \le x \le 0.03$), $MnCoGe_{1-x}In_x$ ($0.005 \le x \le 0.02$), $MnCoGe_x$ ($0.96 \le x \le 0.99$), and $MnCoGe_{1-x}Ga_x$ ($0.04 \le x \le 0.05$). The concurrent magnetic and structural transitions, the so-called magneto-structural transition (T_{mstru}), can lead to giant magnetocaloric effect.[14] Further increasing the amount of the replacements, such as $Mn_{0.97}In_{0.03}CoGe$, results in a further decrease of T_{stru} and a decoupling of magnetic and structural transitions. In this case, the structural transition occurs between FM martensitic and FM austenitic phases with the T_{stru} lower than the T_C of hexagonal austenitic phase. However, the magnetic moment, M_s, of the two phases are quite different due to the different crystal structure. The orthorhombic structure shows a higher M_s ~4.13 μ_B than the hexagonal structure (M_s ~2.76 μ_B).[17]

To precisely learn the details of the lattice change during the phase transition, we performed NPD studies on the variation of crystal and magnetic structures as a function of temperature for some compositions, such as $MnCoGe_{1-x}In_x$ ($x = 0.01, 0.02$), and $MnCoGe_{0.97}Sb_{0.03}$, and the refined results indicate that the differences of lattice volume ($\Delta V/V \sim (V_{ortho} - 2V_{hex})/2V_{hex}$) along with the change of magnetic ordering can be as large as 3.9%, 3.9%, and 3.8%, respectively. We evaluated the linear expansion $\Delta L/L$ and average NTE coefficient $\bar{\alpha}$ from the unit cell parameters for the as-prepared $MnCoGe_{0.99}In_{0.01}$ shown in Figure S1 (NPD results in SI). The linear expansion reaches $\Delta L/L \sim 10995 \times 10^{-6}$ and the average NTE coefficient $\bar{\alpha} \sim -183.3 \times 10^{-6}$/K if we suppose the polycrystalline samples undergo isotropic expansion in the temperature window of phase transition from ~270 to ~330 K (here, the transition window is defined as the region where negative slope of $\bar{V}-T$ occurs, see Figure S1(b)) .

Our $\Delta L/L$ measurements using high-resolution strain gauge indicated that the $\Delta L/L$ behavior is indeed isotropic, independent of the measured axis. Figure 1 shows the $\Delta L/L$

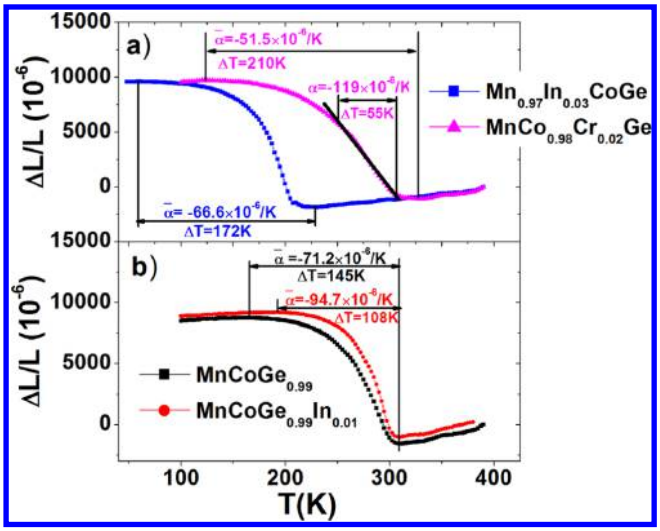

Figure 1. Temperature dependence of linear thermal expansions $\Delta L/L$ (the reference temperature is 390 K) for bonded samples with compositions (a) $Mn_{0.97}In_{0.03}CoGe$, $MnCo_{0.98}Cr_{0.02}Ge$, and (b) $MnCoGe_{0.99}$, $MnCoGe_{0.99}In_{0.01}$.

with respect to the temperature for some typical compositions. The maximal $\Delta L/L$ of 10813, 11715, 11435, 10321, and 10231 × 10^{-6} occurs in a wide temperature window of 210 K (122−332 K), 195 K (122−317 K), 172 K (58−230 K), 145 K (165−310 K), and 108 K (192−310 K), and thus the average linear NTE coefficient reaches −51.5, −60.1, −66.6, −71.2, and −94.7 × 10^{-6}/K for the bonded $MnCo_{0.98}Cr_{0.02}Ge$, $MnCoGe_{0.96}Ga_{0.04}$ (not shown), $Mn_{0.97}In_{0.03}CoGe$, $MnCoGe_{0.99}$, and $MnCoGe_{0.99}In_{0.01}$, respectively. One can notice that the operation temperature region can be tunable from ~60 to ~330 K covering room temperature. Due to the significant broadening of phase transition enforced by residual stress (see following discussion) and the possibly introduced porosities during bonding process (see Figure S3), the measured $\Delta L/L$ and $\bar{\alpha}$ are smaller compared to those estimated from the cell parameters. For example, the measured $\Delta L/L$ amounts to 10231 × 10^{-6} and the $\bar{\alpha}$ reaches -94.7×10^{-6}/K for the bonded $MnCoGe_{0.99}In_{0.01}$, while the estimated ones are $\Delta L/L \sim 10995 \times 10^{-6}$ and $\bar{\alpha} \sim -183.3 \times 10^{-6}$/K from the unit cell parameters for the as-prepared $MnCoGe_{0.99}In_{0.01}$ (NPD results in Figure S1), but the measured maximal $\Delta L/L$ already reaches 93% of the crystallographic value. These novel NTE behaviors, not only the $\bar{\alpha}$ but also the operation-temperature window, exceed the performance of most other materials reported previously. For example, the average $\bar{\alpha}$

DOI: 10.1021/ja510693a
J. Am. Chem. Soc. 2015, 137, 1746−1749

$\sim -51.5 \times 10^{-6}$/K with operation-temperature window as wide as 210 K, appeared in $MnCo_{0.98}Cr_{0.02}Ge$, is more than 5 times larger than that of the commercial NTE materials, i.e., ZrW_2O_8 with $\bar{\alpha} = -9 \times 10^{-6}$/K.[1] More attractively, in the region between 250 and 305 K near room temperature, the α (-119×10^{-6}/K) remains nearly independent of temperature (see Figure 1a). Such a performance is appreciable for practical applications and very similar to the case of the famous material $Bi_{0.95}La_{0.05}NiO_3$.[5] The α value (-119×10^{-6}/K) of the bonded $MnCo_{0.98}Cr_{0.02}Ge$ between 250 and 305 K is ~40% larger than that (-82×10^{-6}/K) of $Bi_{0.95}La_{0.05}NiO_3$ (320 K-380 K)[5] and more than four times larger than the α (-25×10^{-6}/K) reported for the linear expansion of an antiperovskite manganese nitride ceramic (316–386 K).[10]

The observed various NTE coefficients in the bonded MnCoGe-based compounds are mainly caused by the different changing rate of $\Delta L/L$ with respect to temperature, noting the detected maximal $\Delta L/L$ using strain gauge is in the same magnitude, ranging from 10231 to 11715×10^{-6}. Among the five compositions, $MnCo_{0.98}Cr_{0.02}Ge$, $MnCoGe_{0.96}Ga_{0.04}$, $MnCoGe_{0.99}$, and $MnCoGe_{0.99}In_{0.01}$ show similar magnetostructural coupling and behave concurrent magnetic and structural transitions, while $Mn_{0.97}In_{0.03}CoGe$ shows decoupling with separated T_{stru} and T_C.

To reveal the details of structural/magnetostructural (T_{stru}/T_{mstru}) transition and any difference between the bonded and the as-prepared samples, we measured temperature-dependent magnetization ($M-T$ curves) under a magnetic field of 0.3T for the as-prepared and bonded samples, and the representative results are shown in Figure 2a,b, respectively. It can be found that there exists some intrinsic differences in the width of phase transition window besides the different location of T_{stru}/T_{mstru} even for the samples with similar magnetostructural transition, such as $MnCo_{0.98}Cr_{0.02}Ge$, $MnCoGe_{0.99}$, $MnCoGe_{0.99}In_{0.01}$. The size of dM/dT minimum is different from each other, indicating different characteristics of magnetostructural coupling (Figure 2a and its insets). $MnCo_{0.98}Cr_{0.02}Ge$ shows the slowest magnetostructural transformation with respect to temperature, which is in consistent with the widest operation temperature window of the observed NTE behaviors (Figure 1). Generally, the ternary MM′X systems with a hexagonal Ni_2In-type structure exhibit a pronounced wide region of structural transformation (Figure S1). This behavior has been regarded as a character of thermodynamic equilibrium-type martensitic transition in some previous studies.[13] The exact reason for the different width of structural/magnetostructural transition is not clear, but the degree of chemical ordering in the microstructure, caused by the different substitutions on different positions, and its effect on the width of the effective 3d bands and the strength of the covalent bonding should play a dominant role.[13−15]

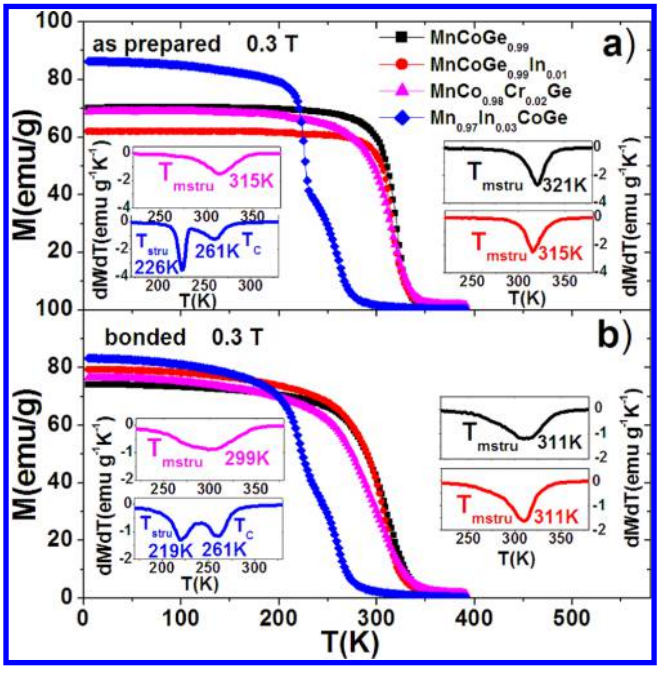

Figure 2. Temperature dependence of magnetization under a magnetic field of 0.3T for (a) as-prepared and (b) bonded samples with compositions $MnCoGe_{0.99}$, $MnCoGe_{0.99}In_{0.01}$, $MnCo_{0.98}Cr_{0.02}Ge$, and $Mn_{0.97}In_{0.03}CoGe$. The insets show the corresponding dM/dT plots.

Furthermore, we find that, from Figure 2a,b, the bonded samples show less sharp structural/magnetostructural transition around the T_{stru}/T_{mstru} and lower T_{stru}/T_{mstru} than the as-prepared samples for every composition, noting the magnitudes of the dM/dT minima and their temperature locations in the insets. For clarity, the compared $M-T$ curves for the bonded and the as-prepared samples are further given for two typical compositions with and without magnetostructural coupling (Figure S2a,b). Significant broadening of structural/magnetostructural transformation can be demonstrated, while the pure magnetic transition width around T_C keeps unchanged for the bonded samples. The T_{mstru} shifts by 10 K (from 321 to 311 K) for the bonded $MnCoGe_{0.99}$ with magnetostructural coupling, while for the decoupled $Mn_{0.97}In_{0.03}CoGe$ with separated T_{stru} and T_C, the T_{stru} shifts by 7 K (from 226 to 219 K), while T_C keeps unchanged (261 K). The bonded samples experienced a high pressure of 11.5 kbar during molding process before solidification at 170 °C. The residual stress in the samples may affect the martensitic structural transformation and round off the structural/magnetostructural transition. For a solid material, a pressure can cause the softening of the acoustic phonon modes and the lattice instability due to the strong electron−phonon coupling.[18] For present systems, the applied physical pressure can tune the martensitic structural transformation and magnetostructural coupling through altering atomic local environments, strength of covalent bonding, and the width of effective 3d bands. It has been reported[14] that applying pressure can drive the T_{mstru} to low temperature for a $Mn_{0.93}Cr_{0.07}CoGe$ compound, and the transition retains sharpness as the pressure is lower than 3.7kbar but notably rounds off as the pressure reaches 5.0 kbar. We carried out the measurements of high-resolution NPD under pressure for the as-prepared $MnCoGe_{0.99}In_{0.01}$. The results directly verified that the transition becomes less sharp as the pressure reaches 6.0 kbar. For the bonded samples, the powders suffer pressures during the molding process, and the residual stress possibly in the grain boundaries and microareas will remain in the resulted samples. In this sense, the residual stress should be largely responsible for the reduction of T_{mstru}/T_{stru} and the notably broadening of the structural/magnetostructural transition. Since the crystallographic component plays a dominant role with magnetic phase transition in a cooperative sense in the MnCoGe-based compounds,[14] the residual stress only affects the T_{mstru}/T_{stru} while has negligible effect on the pure magnetic transition at T_C, noting the shift of T_{mstru}/T_{stru} and the unchanged T_C (Figures 2 and S2 and insets). This should be also the reason that the coupling/decoupling of structural and magnetic transitions does not affect the NET behavior for both the

DOI: 10.1021/ja510693a
J. Am. Chem. Soc. 2015, 137, 1746−1749

magnitude and the width of the operation temperature window (Figure 1).

From an industrial viewpoint, different electrical conductivity is required to meet various applications. The MnCoGe-based compound itself displays good metallic behavior, but the electrical conductivity of the bonded materials can be adjusted through choosing suitable binders. Figure 3a displays the

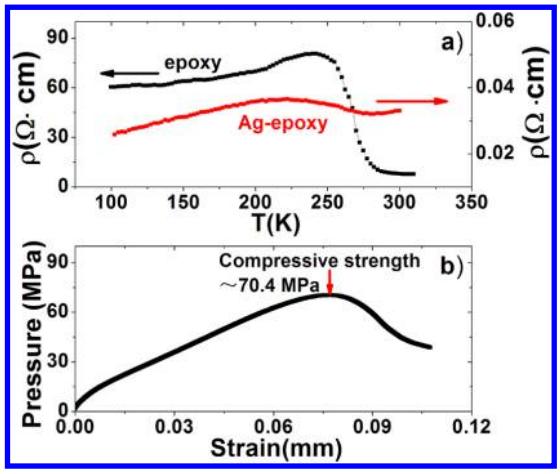

Figure 3. (a) The compared temperature-dependent electrical resistivity for the bonded $MnCoGe_{0.985}In_{0.015}$ with 3.9 wt % epoxy binder and $MnCoGe_{0.99}In_{0.01}$ with 6.0 wt % Ag-epoxy binder. (b) Uniaxial compressive force as a function of strain for a bonded $MnCoGe_{0.99}In_{0.01}$ with 3.9 wt % epoxy-binder.

electrical resistivity as a function of temperature for the bonded $MnCoGe_{0.985}In_{0.015}$ and $MnCoGe_{0.99}In_{0.01}$ with 3.9 wt % epoxy binder and 6.0 wt % Ag-epoxy binder, respectively. One can distinguish the different conductivity behaviors, although the phase transition can still be identified in both cases. The electrical resistivity for the case with Ag-epoxy binder is lower than the case with epoxy binder by 3 orders of magnitude, noting the different vertical scales in Figure 3a. Moreover, we measured the mechanical properties and found that the compressive strength can be as large as 70.4 MPa for a bonded $MnCoGe_{0.99}In_{0.01}$ with 3.9 wt % epoxy binder cooperated (Figure 3b).

In summary, giant NTE has been observed in a number of bonded MnCoGe-based compounds with a Ni_2In-type hexagonal structure. The as-prepared materials are quite brittle. By introducing a few percentages (3−4%) of epoxy to bond the powders and utilizing the significant broadening of phase transition enforced by residual stress, controllable giant NTE has been achieved. For example, the average linear NTE coefficient, $\bar{\alpha}$, as much as -51.5×10^{-6}/K with an operating temperature window as wide as 210 K from 122 to 332 K has been observed in a bonded $MnCo_{0.98}Cr_{0.02}Ge$ compound. Moreover, in the region between 250 and 305 K near room temperature, the α (-119×10^{-6}/K) remains nearly independent of temperature, which is appreciable for practical applications. The bonded materials exhibit excellent mechanical properties and tunable electrical conductivity. All these suggest possible applications as NTE materials, particularly for compensating the materials with high PTE materials, such as the widely used organic or plastic materials.

■ ASSOCIATED CONTENT

Supporting Information

Neutron diffraction measurements; $M-T$ curves; sample bonding process and SEM measurements. This material is available free of charge via the Internet at http://pubs.acs.org.

■ AUTHOR INFORMATION

Corresponding Authors

*fxhu@iphy.ac.cn
*wangjing@iphy.ac.cn

Notes

The authors declare no competing financial interest.

■ ACKNOWLEDGMENTS

This work was supported by the National Basic Research Program of China (973 program, grant nos. 2014CB643702, 2012CB933000), the National Natural Sciences Foundation of China (grant nos. 51271196, 11274357, 11174345), the Beijing Natural Science Foundation (grant no. 2152034), and the Key Research Program of the Chinese Academy of Sciences.

■ REFERENCES

(1) Mary, T. A.; Evans, J. S. O.; Vogt, T.; Sleight, A. W. *Science* **1996**, *272*, 90−92.
(2) Greve, B. K.; Martin, K. L.; Lee, P. L.; Chupas, P. J.; Chapman, K. W.; Wilkinson, A. P. *J. Am. Chem. Soc.* **2010**, *132*, 15496−15498.
(3) Zheng, X. G.; Kubozono, H.; Yamada, H.; Kato, K.; Ishiwata, Y.; Xu, C. N. *Nat. Nanotechnol.* **2008**, *3*, 724−726.
(4) Chen, J.; Nittala, K.; Forrester, J. S.; Jones, J. L.; Deng, J.; Yu, R.; Xing, X. *J. Am. Chem. Soc.* **2011**, *133*, 11114−11117.
(5) Azuma, M.; Chen, W. T.; Seki, H.; Czapski, M.; Olga, S.; Oka, K.; Mizumaki, M.; Watanuki, T.; Ishimatsu, N.; Kawamura, N.; Ishiwata, S.; Tucker, M. G.; Shimakawa, Y.; Attfield, J. P. *Nat. Commun.* **2011**, DOI: 10.1038/ncomms1361.
(6) Iikubo, S.; Kodama, K.; Takenaka, K.; Takagi, H.; Takigawa, M.; Shamoto, S. *Phys. Rev. Lett.* **2008**, *101*, 205901.
(7) Sun, Y.; Wang, C.; Huang, Q.; Guo, Y.; Chu, L.; Arai, M.; Yamaura, K. *Inorg. Chem.* **2012**, *51*, 7232−7236.
(8) Song, X.; Sun, Z.; Huang, Q.; Rettenmayr, M.; Liu, X.; Seyring, M.; Li, G.; Rao, G.; Yin, F. *Adv. Mater.* **2011**, *23*, 4690−4694.
(9) Nakamura, Y.; Takenaka, K.; Kishimoto, A.; Takagi, H. *J. Am. Ceram. Soc.* **2009**, *92*, 2999−3003.
(10) Takenaka, K.; Takagi, H. *Appl. Phys. Lett.* **2005**, *87*, 261902.
(11) Huang, R. J.; Liu, Y. Y.; Fan, W.; Tan, J.; Xiao, F. R.; Qian, L. H.; Li, L. F. J. *Am. Chem. Soc.* **2013**, *135*, 11469−11472.
(12) Niziol, S.; Weselucha, A.; Bazela, W.; Szytula. *Solid State Commun.* **1981**, *39*, 1081−1085.
(13) Liu, E. K.; Wang, W. H.; Feng, L.; Zhu, W.; Li, G. J.; Chen, J. L.; Zhang, H. W.; Wu, G. H.; Jiang, C. B.; Xu, H. B.; de Boer, F. *Nat. Commun.* **2012**, *3*, 873.
(14) Caron, L.; Trung, N. T.; Bruck, E. *Phys. Rev. B* **2011**, *84*, 020414−020417.
(15) Gercsi, Z.; Hono, K.; Sandeman, K. G. *Phys. Rev. B* **2011**, *83*, 174403.
(16) Larson, A. C.; Von Dreele, R. B. General Structure Analysis System (GSAS). *Report LAUR 86-748*; Los Alamos National Laboratory: Los Alamos, NM, 2000.
(17) Wang, J. T.; Wang, D. S.; Chen, C. F.; Nashima, O.; Kanomata, T.; Mizuseki, H.; Kawazoe, Y. *Appl. Phys. Lett.* **2006**, *89*, 262504−262506.
(18) Luo, W.; Ahuja, R.; Ding, Y.; Mao, H. K. *Proc. Natl. Acad. Sci. U.S.A.* **2007**, *104*, 16428−16431.

DOI: 10.1021/ja510693a
J. Am. Chem. Soc. 2015, 137, 1746−1749